www.cadanda.com
Computer-Aided Design AND APPLICATIONS

Implications for English Teaching Expert System Human-Computer Interaction Based on Artificial Intelligence and Improved Machine Learning Algorithm

Hui Chen[1*]

[1]Hunan University of Information Technology, Changsha, 410151, Hunan, China

Corresponding Author: Hui Chen, Chxxxy3130@163.com

Abstract. This paper presents a novel approach to enhancing the intelligent effect of English teaching. We have developed an English teaching expert system integrated with e-commerce by combining artificial intelligence and advanced machine learning algorithms. This system not only enhances the intelligence of English teaching but also carries out intelligent image recognition and data analysis. Our research methodology involved simulation to verify the behavior of the English teaching image unit under strain and the influence of cavity length on the reflection spectrum of the English teaching image unit. The results of our simulation research conclude that to ensure the fineness of the reflection spectrum of the microcavity unit, the cavity length should be as much as possible to be greater than or equal to the grating length. The experiment shows that with the improvement of the intelligence of the expert system, there is a positive correlation between the English teaching effect and the intelligence of the specialist system so that the expert system can play an important role in English teaching.

Keywords: Artificial intelligence; machine learning; improved algorithm; English teaching; expert system; Human-computer Interaction
DOI: https://doi.org/10.14733/cadaps.2025.S6.72-87

1 INTRODUCTION

Education and teaching workers at home and abroad have continued pursuing effective teaching in ancient and modern times. However, what effective teaching is, how to achieve effective teaching, how to evaluate the effectiveness of teaching, and other issues are still pending. In recent years, the hot topics of "effective teaching" research mainly include the nature of effective teaching, the characteristics and methods of effective teaching, the factors affecting effective teaching, the behavioral judgment of effective teaching, the strategies of effective teaching, and the evaluation criteria of effective teaching, etc. The research has involved all aspects of "effective teaching," and some scholars even proposed that the research of "effective teaching" will drive or even impact the theoretical research and reform practice at the macro, meso, and micro levels of education [15]. The so-called "effective teaching" means that teachers make students achieve specific progress or

development after a teaching period. Whether students have progress or development is the only indicator of effective teaching. Usually, the so-called "effective teaching" refers to the effectiveness of classroom teaching, a narrow concept [6]. Some scholars have proposed that "effective teaching" can fully open up the practice space of the "teacher research community." This is because, fundamentally speaking, not every teacher but the entire team of teachers undertakes the learning and development of students; not every classroom, but the whole school [3]. A "teacher research community" is a community that transcends disciplines, classrooms, and schools and is closely connected with the entire society and the whole world [8].In other words, the realization of effective teaching is not limited to a specific classroom or classroom but any place where learning takes place under the guidance of the "teacher." Ineffective teaching, a "teacher" can be not only a team that transcends individuals but also a "smart" computer" that transcends human beings, that is, a teaching expert system [9].

The micro-course-based teaching expert system takes knowledge points as the core, establishes a student model by testing students' learning styles and related topics, and obtains the cognitive structure of each student's different learning style tendencies and associated topics. Incorporating Human-Computer Interaction (HCI) principles ensures that the system is user-friendly and effectively engages students. Additionally, integrating e-commerce elements can facilitate the distribution and monetization of educational resources, allowing for a seamless and efficient learning experience tailored to individual needs. This approach enhances the system's usability through HCI and leverages e-commerce strategies to support and expand educational opportunities. Based on this, the teaching expert system should automatically call or let students choose the corresponding "micro-course" teaching materials according to specific teaching strategies [11]. The "micro-course" is designed based on different teaching strategies and is an optimized resource for students to carry out individualized learning. At the same time, the teaching expert system also has "the ability to grow, amend and construct knowledge and strategies." For the teacher-student relationship. This kind of judgment based on the starting point of learning makes students' learning goals clear, can effectively expand and improve students' cognitive structure, and highlights the effect of learning [14].

Suppose the teaching strategy library material of the traditional teaching expert system needs to use the support of teaching experts. In that case, it is usually an audio teaching video organized and presented in one lesson (45 or 50 minutes) as a unit of time. This "original" teaching material is precious. Still, it needs to be more universal because it pays too much attention to the integrity of the classroom, and it is indeed a challenging task for students to insist on learning such long content [7]. In response to the different needs of different students for learning content, the teaching expert system uses the "micro-learning" theory to "fragment the complete knowledge," and each fragmented "knowledge fragment" is relatively independent and corresponds to several "knowledge fragments" with different characteristics. Micro-courses" (usually 1-3 minutes) to meet the cognitive characteristics and learning styles of other students. This kind of teaching expert system based on "micro-courses" can truly achieve one-to-many and improve teaching efficiency. At the same time, using "fragments" to "seamlessly connect" with students' cognitive deficits can enhance the efficiency of students' learning [1].

Mobile learning indicates the birth of a new learning model and a new way of life for people in the information age. The teaching expert system based on "micro-course" is like an experienced teacher who solves the confusion caused by the student's learning process in real time. To achieve a student-centered, computer-mediated, open interactive teaching process [5]. The "small and specialized" characteristics of micro-courses are especially suitable for mobile learning in complex environments, which can highlight that "education is life, and learning is dialogue and communication." This new learning resource and environment, which is very close to modern life, will make students feel more friendly and more likely to stimulate their learning interests and autonomy, thereby improving learning efficiency [10].

The Intelligent Teaching Expert System (ITES) is an open human-computer interaction teaching system developed by introducing artificial intelligence technology to organically combine subject-expert knowledge and computer-aided education. Incorporating Human-Computer Interaction (HCI) principles ensures that the ITES is user-friendly and effectively engages learners. Additionally, integrating e-commerce elements can facilitate the distribution and monetization of educational resources, making it easier to access and purchase educational content. This approach enhances the system's usability through HCI and leverages e-commerce strategies to support and expand educational opportunities. Mainly comprises four parts: a teaching module, an expert module, a student module, and a user interface module [2]. ITES is a subject expert consultation system. It has the reasoning and solving functions of ordinary expert systems and the ability to understand and answer students' learning situations, establish student files, and guide students' learning, thus enriching the teaching experts. Experience and profound knowledge can be promoted. To achieve the update and development of teaching methods [12]. How to build a perfect ITES, how to make the intelligent system have expert knowledge, or how to make the teaching experts and the computer "knowledge exchange" (this process is called knowledge processing), this is the key to the establishment of ITES [16]. The performance of the expert system depends on expert knowledge, so knowledge processing in ITES is essential; it is related to the quality or success or failure of ITES. Knowledge processing is to regularize, quantify, and formalize (symbolize) the rich knowledge of teaching experts so that computers can understand and accept them. Then, they generate teaching strategy rules, form models, and complete the teaching process. According to the principle of knowledge engineering, the knowledge processing of teaching expert systems includes three processes: knowledge representation, knowledge acquisition, and knowledge management [13].

Expert system programming is a branch of artificial intelligence. Expert systems are one of the most successful fields of artificial intelligence applications, and they have been widely used in solving unstructured problems in recent years. The system stores the knowledge of human experts in the professional field in the computer program, enabling the computer to solve specific problems at a level close to or equivalent to an expert within a particular range [17]. The experimental course of expert system programming has always been compulsory for students majoring in artificial intelligence in colleges and universities. Students often can only follow the script for the theory, lacking their own opinions. The traditional teaching mode of colleges and universities is facing challenges, and the guiding policy has changed from the education method that emphasizes theory and practice to the direction that emphasizes innovation and training [4]. In this context, analyzing the experimental content and curriculum construction of the expert system in universities helps discuss the reform of experimental teaching in the curriculum construction in colleges and universities. It has a positive effect on cultivating students' innovation and application ability [18].

This paper combines artificial intelligence and improved machine learning algorithms to enhance the intelligence of the English teaching expert system and improve the quality of English teaching.

2 INTELLIGENT ALGORITHM OF ENGLISH TEACHING IMAGE RECOGNITION

2.1 Intelligent Algorithm of English Teaching Image Recognition

The structural parameters of fiber Bragg gratings mainly include the length of the light gate, the grating period, and the depth of refraction modulation. In the practical application system, gratings with different parameters will be selected according to the test needs, and the spectral characteristics of the FBG will be analyzed in combination with the coupling mode equation.

For ordinary single-mode FBGs, coupling occurs between the forward and backward transmission modes with wavelengths close to the Bragg wavelength. According to the coupled mode theory, the following coupling mode equation can be obtained:

$$\left.\begin{array}{l}\dfrac{dA\ z}{dz}=iKB\ z\ \exp\ -2i\ \Delta\beta\ z\\ \dfrac{dB\ z}{dz}=-iKA\ z\ \exp\ 2i\ \Delta\beta\ z\end{array}\right\}\quad 0\le z\le L \tag{1}$$

In the formula, L represents the grating length, 4β represents the Bragg wavelength vector distribution, K represents the transverse coupling coefficient, A(=) represents the forward transmission mode amplitude, B(z) represents the backward transmission mode amplitude, and $\Delta\beta=\beta-\beta_0=2\pi n_{eff}/\lambda-\pi/$. Among them, $_{Neff}$ is the effective refractive index of the fiber, A is the grating period, λ is the center wavelength of the grating, and the transverse coupling coefficient is:

$$K=\frac{\pi\Delta n}{\lambda} \tag{2}$$

Therefore, according to equation (1), we can get:

$$\left.\begin{array}{l}A\ z\\ =A_0e^{-i\beta z}\dfrac{-i\Delta\beta\sin hS\ \ L-z\ \ +S\cos hS\ \ L-z}{S\cos hSL+i\Delta\beta\sin hSL}\\ +B_Le^{-i\beta z}\dfrac{e^{-i\beta z}}{KsinSL}\left[-S\dfrac{-i\Delta\beta\sin hS\ \ L-z\ \ +S\cos hS\ \ L-z}{S\cos hSL+i\Delta\beta\sin hSL}\right]\\ -i\ \ i\Delta\beta\sin hSz+iS\cos hSz\end{array}\right\} \tag{3}$$

$$\left.\begin{array}{l}B\ z\\ =A_0e^{-i\beta z}\left[-\dfrac{K\sin hS\ \ L-z}{S\cos hSL+i\Delta\beta\sin hSL}\right]\\ +B_Le^{-i\beta z}\left[\dfrac{e^{-i\beta z}}{\sin hSL}\left(\dfrac{S\sin hS\ \ L-z}{S\cos hSL+i\Delta\beta\sin hSL}\right)\right]\\ +\sin hSz\end{array}\right\} \tag{4}$$

Among them, S satisfies the relation:

$$S^2=K^2-\Delta\beta \tag{5}$$

If the input light intensity amplitude is assumed to be 1, according to the boundary conditions of the coupled mode theory: A(0)=1, B(L)=0, by combining formulas (3) and (4), the reflection coefficient and transmission coefficient of the grating can be obtained as:

$$r\ \lambda\ =\frac{B\ 0}{A\ 0}=\frac{-K\sin h\ \ SL}{\Delta\beta\sin h\ \ SL\ \ +iS\cos h\ \ SL} \tag{6}$$

$$t\ \lambda\ =\frac{A\ L}{A\ 0}=\frac{S}{\Delta\beta\sin h\ \ SL\ \ -iS\cos h\ \ SL} \tag{7}$$

From formulas (6) and (7), the reflectivity and transmittance of the grating can be obtained as:

$$R\ \lambda\ = \left| r\ \lambda\ \right|^2 = \frac{-K \sin h^2\ \ SL}{\Delta\beta^2 \sin h^2\ \ SL\ + S^2 \cos h^2\ \ SL} \tag{8}$$

$$T\ \lambda\ = \left| t\ \lambda\ \right|^2 = \frac{S^2}{\Delta\beta^2 \sin h^2\ \ SL\ + S^2 \cos h^2\ \ SL} \tag{9}$$

From formulas (8) and (9), it can be obtained that when $\Delta\beta = 0$, the grating has the maximum reflectivity and the minimum transmittance, respectively:

$$R \tan h^2\ \ KL\ _{max} \tag{10}$$

$$T \cos h^{-2}\ \ KL\ _{min} \tag{11}$$

At this time, the center wavelength λ_B of the grating is:

$$\lambda_B = 2n_{eff} \tag{12}$$

It can be known from formula (8) that when $SL = \pm k\pi$, The reflectivity of the FBG reflection spectrum is 0. It can be obtained that the zero-point bandwidth $\Delta\lambda_0$ of the grating is:

$$\Delta\lambda_0 = \frac{\lambda \cdot \Delta n}{n_{eff}} \sqrt{1 + \left(\frac{\lambda_B}{\Delta n \cdot L} \right)} \tag{13}$$

For weak gratings with minimal refractive index modulation depths, $\Delta n = \lambda_B / L$, so:

$$\Delta\lambda_0 = \frac{\lambda_B \cdot \lambda}{n_{eff} L} = \frac{2n_{eff} \wedge \lambda}{L} \tag{14}$$

When the grating length is constant, the greater the refractive index modulation depth, the stronger the reflection. When the refractive index modulation depth is continuous, the longer the grating length, the narrower the spectral width, and the stronger the reflectivity. Therefore, conventional weak grating arrays cannot simultaneously meet the requirements of spatial resolution and detection accuracy.

Given the detection requirements of long distance, high spatial resolution, high precision, and complete distribution in surface morphology perception, if the ultra-short grating array is used to detect the spatial discrete curvature, it will lead to problems of spectral broadening and reflectivity decline, and the grating interval will cause a detection blind area. Therefore, this Project uses microcavity array fiber to meet the detection requirements.

The microcavity array fiber is essentially an isotonic grating array structure, and its structure diagram is shown in Figure 1. A microcavity (MC) is formed by two adjacent ultra-short gratings, FBG#1 and FBG#2. The interval between the gratings together forms MC#1. Moreover, FBG#n and FBG#n+1 and the spacing between the gratings constitute MCl#n.

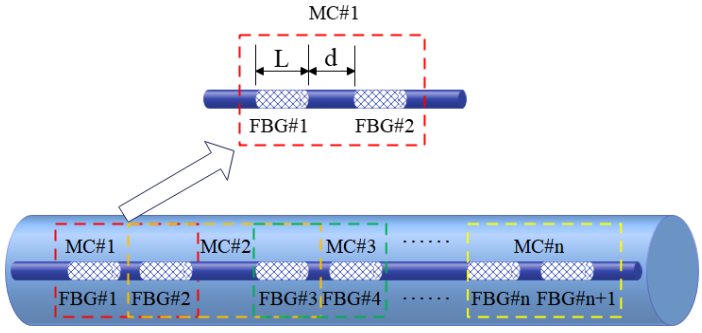

Figure 1: Structure diagram of microcavity array fiber.

We need to analyze its sensing characteristics to utilize the microcavity unit for sensing better. Each microcavity unit can be regarded as a series of two gratings and a section of optical fiber. Therefore, the reflection spectrum of the entire microcavity can be calculated through the transmission matrix.

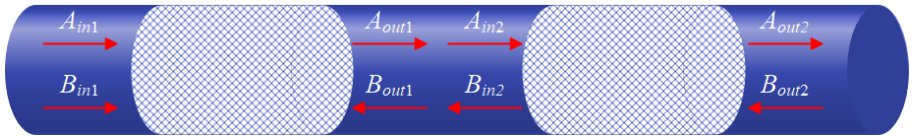

Figure 2: Schematic diagram of light propagation in the microcavity unit.

As shown in Figure 2, in the microcavity unit MC#1, it is assumed that the forward and backward reflection coefficients and transmission coefficients of FBG#1 are r_1, r_1', t_1, t_1' respectively, so the transmission matrix TFscwn of FBG#1 can be obtained to satisfy the following relationship:

$$\begin{bmatrix} 1 \\ r_1 \end{bmatrix} = T \begin{bmatrix} t_1 \\ 0 \end{bmatrix} \begin{bmatrix} 1 \\ t_1' \end{bmatrix} = T \begin{bmatrix} r_1' \\ 0 \end{bmatrix} \tag{15}$$

By solving formula (15), we can get:

$$T_{FBG\#1} = \frac{1}{t_1} \begin{bmatrix} 1 & -r_1' \\ r_1 & t_1 t_1' - r_1 r_1' \end{bmatrix} \tag{16}$$

Similarly, if the forward and backward reflection coefficients and transmission coefficients of FBG#2 are set to be r_1, r_1', t_1, t_1', respectively, then the transmission matrix $T_{FBG\#2}$ of FBG#2 satisfies the following relationship:

$$T_{FBG\#2} = \frac{1}{t_2} \begin{bmatrix} 1 & -r_2' \\ r_2 & t_2 t_2' - r_2 r_2' \end{bmatrix} \tag{17}$$

For the single-mode fiber with the cavity length d of the microcavity unit, the light wave only changes the phase, so its transmission matrix can be expressed as TF:

$$T_F = \begin{bmatrix} P & 0 \\ 0 & P^{-1} \end{bmatrix} \tag{18}$$

Among them, $P = \exp\ j\beta d$ and $\beta = 2\pi n_{eff} / \lambda$, so the transmission matrix T_{MC} of the entire microcavity unit satisfies the following relationship:

$$\begin{pmatrix} A_{in1} \\ B_{out1} \end{pmatrix} = T_{mc} \begin{pmatrix} A_{out2} \\ B_{in2} \end{pmatrix} = \frac{1}{t_1 t_2} \begin{bmatrix} 1 & -r_1^{'} \\ r_1 & t_1 t_1^{'} - r_1 r_1^{'} \end{bmatrix} \begin{bmatrix} P & 0 \\ 0 & P^{-1} \end{bmatrix} \begin{bmatrix} 1 & -r_2^{'} \\ r_2 & t_2 t_2^{'} - r_2 r_2^{'} \end{bmatrix} \begin{pmatrix} A_{out2} \\ B_{in2} \end{pmatrix} \tag{19}$$

By simplification, we get:

$$T_{MC} = \begin{bmatrix} T_{11} & T_{12} \\ T_{21} & T_{22} \end{bmatrix} = \begin{bmatrix} P / \ t_1 t_2 \ + r_2 r_1^{'} & \mathrm{Pr}_2^{'} / \ t_1 t_2^{'} \ + r_1^{'} / \ P t_2^{'} t_1^{'} \\ \mathrm{Pr}_1 / \ t_1 t_2 \ + r_2 / \ P t_2 t_1^{'} & \mathrm{Pr}_1 r_2^{'} / \ t_1 t_2^{'} \ + 1 / \ P t_2^{'} t_1^{'} \end{bmatrix} \tag{20}$$

Therefore, the amplitude transmission coefficient of the microcavity unit can be expressed as:

$$t_{MC} = \frac{1}{T_{11}} = \frac{t_1 t_2}{1 - r_1 r_2 \exp\ i2\beta d} \tag{21}$$

The transmission spectrum T_{MC} is:

$$T_{MC} = \left| t_{MC} \right|^2 = \frac{\left| t_1 \right|^2 \left| t_2 \right|^2}{1 + \left| r_1 \right|^2 \left| r_2 \right|^2 - 2\left| r_1 \right| \left| r_2 \right| \cos\ 2\beta d - \varphi_{r1} - \varphi_{r2}} \tag{22}$$

If it is assumed that in the microcavity unit, the parameters of the two FBGs are precisely the same, that is, $r_1 = r_2 = \left| r \right| \exp\ i\varphi_{r1}$ and $t_1 = t_2 = \left| t \right| \exp\ i\varphi_{r1}$, Then formula (22) can be expressed as:

$$T_{MC} = \left| t_{MC} \right|^2 = \frac{1}{1 + F \sin^2\ \beta d - \varphi_r} \tag{23}$$

In the formula, $F = 4\left| r \right|^2 / \left[1 - \left| r \right|^2 \right]^2$ represents the fineness of the fringes. Similarly, the reflectivity of the microcavity unit is expressed as:

$$R_{MC} = \frac{T_{21}}{T_{11}} = \frac{F \sin^2\ \beta d - \varphi_r}{1 + F \sin^2\ \beta d - \varphi_r} = \frac{F \sin^2 \left(\frac{\varphi_r}{2} - \varphi_r \right)}{1 + F \sin^2 \left(\frac{\varphi_r}{2} - \varphi_r \right)} \tag{24}$$

Represents the phase delay formed by the interval between the microcavity units and satisfies $\varphi = 2\beta d = 4\pi n_{eff} / \lambda d$. According to the above analysis, we simulated and analyzed the reflection spectrum of the microcavity unit composed of two gratings with a length of 1mm, an interval of 2mm, a center wavelength of 1550nm, and a reflectivity of 1/10,000, as shown in Figure 3. The red

spectrum is the reflectance spectrum of the microcavity unit, and the blue spectrum is the reflectance spectrum of a single FBG.

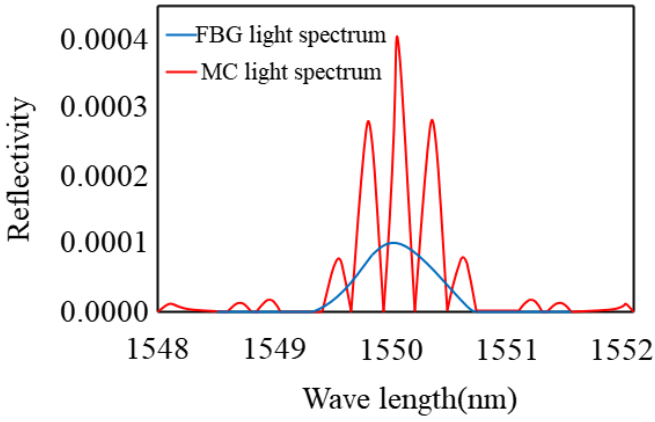

Figure 3: Simulation diagram of the reflection spectrum of the microcavity unit.

When the reflectivity of the two gratings is <<1, there is an approximate relationship as follows:

$$\varphi - \varphi_r \approx 4\pi n_{eff} \ L + d \ / \lambda \tag{25}$$

Combined with formula (8), formula (24) can be simplified as:

$$R_{MC} = 2R \ \lambda \left\{1 + \cos\left[\frac{4\pi n_{eff} \ L + d}{\lambda}\right]\right\} \tag{26}$$

It can be known from equation (26) that the reflection spectrum of the microcavity unit consists of two parts. The first part is the envelope formed by the grating itself. The second part is $1 + \cos\left[4\pi n_{eff} \ L + d \ / \lambda\right]$, Corresponding to the interference fringes of the reflection spectrum of the microcavity unit. From the zero-point bandwidth of the grating in equation (13), the resonant spectral line bandwidth of the microcavity unit can be obtained as:

$$\Delta\lambda_n = \frac{\lambda^2}{2n_{eff}d} \tag{27}$$

Therefore, the number of resonance lines in the reflection spectrum of the microcavity unit is:

$$m = \frac{\Delta\lambda_0}{\Delta\lambda_n} \approx \frac{2d}{L} \tag{28}$$

According to formula (28), in the microcavity unit, the cavity length d should be made more significant than the gate length L as much as possible to form more resonance peaks in the reflection spectrum range. To verify the above conclusion, we simulated the reflection spectrum under constant gate length and different cavity lengths according to equation (24). The shed length is 1mm, the center wavelength is 1550nm, the reflectivity is 1/10,000, and the cavity lengths are set to 1mm, 2mm, 4mm, 6mm, and 8mm, respectively. It can be seen from Figure 4 that as the cavity length d

increases, the number of resonance peaks increases, the interval between the resonance peaks decreases, and the spectral peak reflectivity remains unchanged.

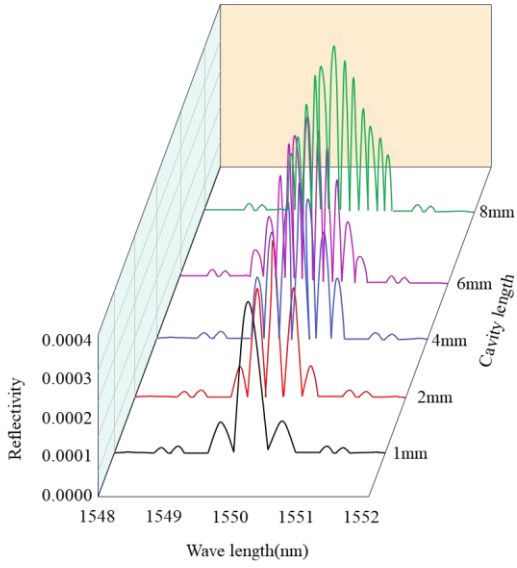

Figure 4: Reflection spectra of microcavity elements with different cavity lengths.

To facilitate the analysis of the microcavity unit's sensing characteristics, we set the sensing parameters of the two gratings to be the same. Next, starting from the grating's sensing characteristics, the strain-sensing characteristics of the microcavity unit will be analyzed.

According to the Bragg formula of formula (12), it can be known that the response of the change of the center wavelength of the grating, temperature, and strain is:

$$\frac{\Delta\lambda_B}{\lambda_B} = \frac{\Delta n_{eff}}{n_{eff}} + \frac{\Delta\wedge}{\wedge} = \left(1 - P_e\right)\Delta\varepsilon + \left(\alpha + \xi\right)\Delta T \tag{29}$$

In the formula, P_e is the effective elastic-optic coefficient, $\Delta\varepsilon$ is the strain change experienced by the grating, ΔT is the temperature change experienced by the grating, α is the thermal expansion coefficient of the fiber, and ξ is the thermo-optic coefficient of the fiber. For conventional single-mode fibers, Pe≈0.22 is generally taken. Since temperature and strain have the same effect on the wavelength change of the grating, the strain will be analyzed below.

For a single grating, when only stressed, the phase change of the microcavity unit can be expressed as:

$$\Delta\varphi = \frac{4\pi n}{\lambda_B}\Delta L + \frac{4\pi n}{\lambda_B}\Delta n + \frac{4\pi nL}{\lambda_B^2}\Delta\lambda_B \tag{30}$$

Therefore, the relative amount of phase change can be expressed as:

$$\frac{\Delta\varphi}{\varphi} = \frac{\Delta L}{L} + \frac{\Delta n}{n} - \frac{\Delta\lambda_B}{\lambda_B} = \left(1 - P_e\right)\Delta\varepsilon - \frac{\Delta\lambda_B}{\lambda_B} \tag{31}$$

Combining formula (29), we can get:

$$\frac{\Delta\varphi}{\varphi} = 0 \tag{32}$$

Therefore, it can be seen that when the microcavity unit is subjected to stress, the spectrum of the grating does not change in phase. In this regard, we also conducted a simulation verification analysis. We set the gate length L as 1mm, the cavity length d as 2mm, the initial center wavelength at 1550nm, and the reflectivity at 1/10,000. Moreover, we assume that the simulated spectrum is shown in Fig. 5 when a strain of 100 ue is applied across the microcavity unit. It can be seen that when the strain of the microcavity unit occurs, the spectrum will only shift as a whole but will not change the phase.

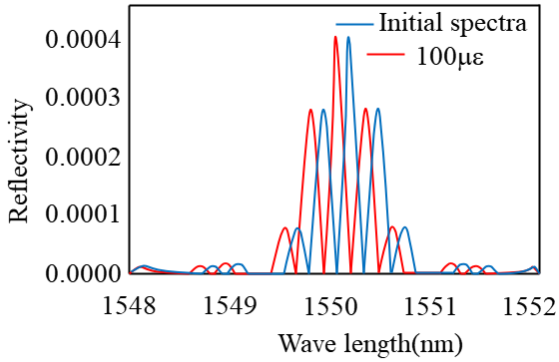

Figure 5: Reflection spectrum of microcavity unit under strain.

2.2 Curvature Information Acquisition Based on Microcavity Array Fiber

The shape perception of the three-dimensional space surface can be realized based on the spatial discrete curvature information. Hence, acquiring the spatial curvature information becomes one of the critical links to discovering the surface shape perception. To establish the relationship between the wavelength change and the curvature information of the microcavity unit, we establish a mechanical structure model and obtain the relationship between the wavelength change and the spatially discrete curvature according to the flexible bending theory.

We assume no internal tangential strain exists in the entire microcavity unit structure. The temperature remains constant, and the microcavity unit is only subjected to axial tension or compression. According to formula (30), the wavelength and strain of the microcavity unit satisfy the following relationship:

$$\frac{\Delta\lambda_{MC}}{\lambda_{MC}} = 1 - P_e \ \varepsilon \tag{33}$$

In the formula, $\Delta\lambda_{MC}$ is the wavelength variation of the microcavity unit, and λ_{MC} is the center wavelength of the microcavity unit.

We assume that the microcavity structure is pasted on the substrate, the substrate is a beam-like structure of equal cross-section, and the microelement structure with length l and thickness h is intercepted, as shown in Fig. 6(a). Moreover, if the substrate is assumed to satisfy the ideal

deformation conditions, there is a central plane when the substrate is bent, as shown by the dashed line in Fig. 6(b). In the lower half of the neutral plane, that is, the inside of the substrate, the substrate is compressed and shortened when bending occurs.

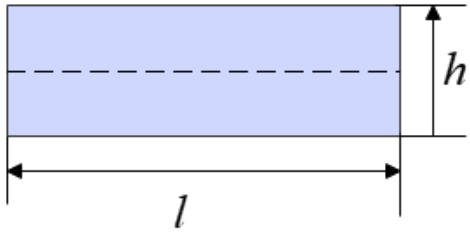

(a) Base material before blending

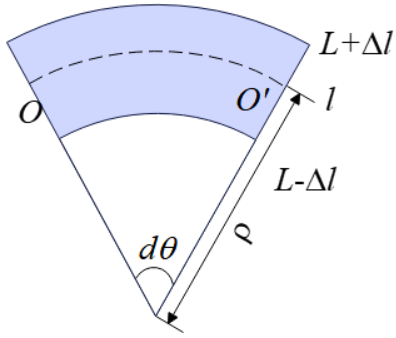

(b) Base material after blending

Figure 6: Schematic diagram of substrate bending.

It can be seen from the above figure and the arc length formula:

$$l = \rho \cdot d\theta \tag{34}$$

$$l + \Delta l = \left(\rho + h/2\right) \cdot d\theta \tag{35}$$

$$\varepsilon = \frac{\Delta l}{l} \tag{36}$$

Combining formulas (34) and (35), we can get:

$$k = \frac{1}{\rho} = \frac{2\Delta l}{hl} = \frac{2}{h}\varepsilon \tag{37}$$

In the above formula, k represents the bending curvature of the substrate, c represents the strain value of the substrate, 4I represents the length change of the substrate, and h represents the thickness of the substrate. By substituting formula (33) into formula(37), we get:

$$k = \frac{2\Delta\lambda_{MC}}{\lambda_{MC}\ 1-P_c\ h} \tag{38}$$

We assume that K satisfies the following relation:

$$k = \frac{2}{\lambda_{MC}\ 1-P_c\ h} \tag{39}$$

At this time, the curvature k can be expressed as:

$$k = K \cdot \Delta\lambda_{MC} \tag{40}$$

Therefore, it can be known from the above formula that a linear relationship is satisfied between the curvature k of the substrate and the wavelength change $\Delta\lambda_{MC}$ of the microcavity unit. For the packaged microcavity unit structure, the initial wavelength of the microcavity unit is λ_{MC}, and the thickness h of the substrate and the effective elastic-optic coefficient P_e are both constants. The substrate's curvature can be obtained only by detecting the rate of change of the central wavelength of the microcavity unit, thereby providing essential data for the subsequent perception of surface shape.

In the actual application process, since the spatial discrete curvature detected by the microcavity unit has a specific interval, to make the restored spatial surface shape smoother, it is necessary to use an interpolation algorithm to obtain more discrete curvature information so that the detected curvature information is continuous to a certain extent. To improve the efficiency of the algorithm operation, the research group adopts the linear interpolation algorithm to realize the continuity of the surface space's curvature without affecting the surface reconstruction's smooth accuracy.

We assume an arc length s and a linear relationship between arc length s and curvature k. Then, it can be expressed as:

$$k = x \cdot s + y \tag{41}$$

Among them, x and y are the constants to be determined. If two adjacent discrete curvatures are detected as k_1 and k_2, and the arc positions where they are located are s_1 and s_2, respectively, the following relationship exists:

$$\begin{cases} k_1 = x \cdot s_1 + y \\ k_2 = x \cdot s_2 + y \end{cases} \tag{42}$$

Therefore, the slope x and intercept y can be obtained as:

$$\begin{cases} x = k_2 - k_1\ /\ s_2 - s_1 \\ y = k_1 \cdot s_2 - k_2 \cdot s_1\ /\ s_2 - s_1 \end{cases} \tag{43}$$

Substituting formula (43) into formula (41), we can get:

$$k = s \cdot\ k_2 - k_1\ /\ s_2 - s_1\ +\ k_1 \cdot s_2 - k_2 \cdot s_1\ /\ s_2 - s_1 \tag{44}$$

Therefore, the continuation of discrete curvatures can be achieved by formula (44).

This paper considers the beam energy problem in fabricating microcavity array fibers to ensure the sensing system's high spatial resolution and detection length. Moreover, the research group adopts a grating array with an interval of 0.5mm, a grating length of 0.5mm, and a reflectivity of -45dB to form a microcavity array fiber to realize the detection of spatial curvature.

3 ENGLISH TEACHING EXPERT SYSTEM BASED ON ARTIFICIAL INTELLIGENCE AND IMPROVED MACHINE LEARNING ALGORITHM

The working flow chart of the dynamic self-optimization system in the teaching process is shown in Figure 7.

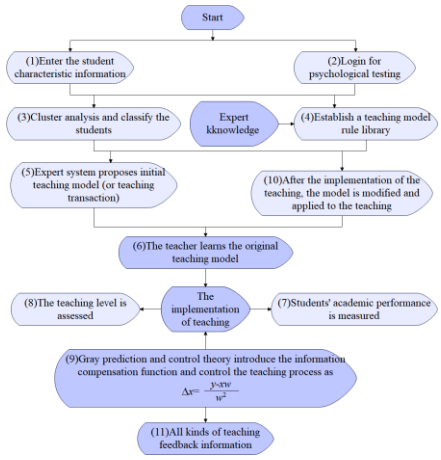

Figure 7: Workflow of the expert system.

The reasoning engine design of the English teaching expert system is based on fuzzy reasoning, reasoning combined with an artificial neural network model, non-monotonic reasoning mixed control strategy, and other reasoning mechanisms. The reasoning engine matches the rules in the knowledge base according to the conditions or known information of the problems in English reading teaching. It obtains new conclusions to solve the results. The reasoning network drawn in Fig. 8 helps teachers and students understand the reasoning and interpretation mechanisms of the expert system.

After constructing the English teaching expert system based on artificial intelligence and an improved machine learning algorithm, the effect of the English expert teaching system proposed in this paper is verified, and the results shown in Figure 9 are obtained. Figure 9 shows that as the intelligence of the expert system improves, there is a positive correlation between the English teaching effect and its intelligence so that the expert system can play an important role in English teaching.

4 CONCLUSIONS

The design and implementation of knowledge representation, knowledge acquisition, and knowledge management processes in knowledge processing of intelligent teaching expert systems lay the foundation for the development of ITES. With the development and progress of computer science, especially in recent years, with the application of MAS, Web technology, knowledge management, data mining, ontology, network technology, etc., in ITES, the architecture of ITES has made new progress.

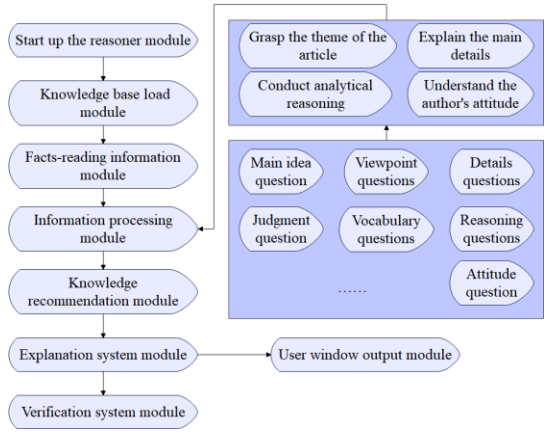

Figure 8: Reasoning network of English teaching expert system.

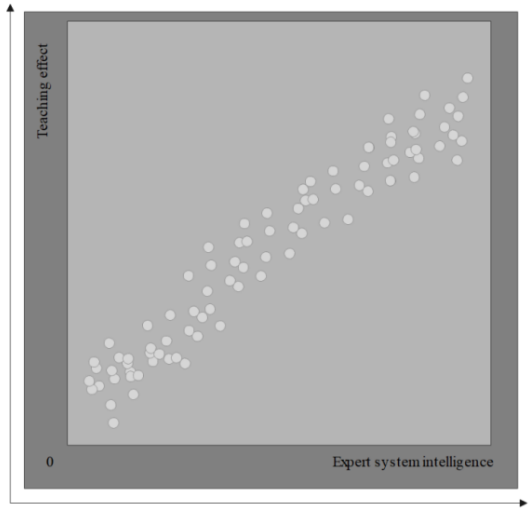

Figure 9: Teaching effect of English teaching expert system.

Moreover, ITES based on MAS (Multi-Agent System), ITES based on the Web, ITES based on Grid (Grid), and ITES based on CSCL (Computer Supported Collaborative Learning) have appeared. This paper combines artificial intelligence and improved machine learning algorithms to enhance the intelligence of the English teaching expert system and improve the quality of English teaching. The fusion of AI, enhanced machine learning, e-commerce, and Human-Computer Interaction (HCI) within an English teaching platform represents an innovative approach to customized language education. Employing a structured methodology can reshape the learning environment, providing interactive lessons, personalized feedback, and avenues for revenue generation through e-commerce. Upholding legal compliance and ongoing maintenance is essential for sustained relevance, ultimately promising heightened accessibility and effectiveness in language learning endeavors. Integrating e-commerce strategies ensures that educational resources are readily

available for purchase, while HCI principles enhance user engagement and the overall learning experience. The experiment shows that with the improvement of the intelligence of the expert system, there is a positive correlation between the English teaching effect and the intelligence of the specialist system so that the expert system can play an important role in English teaching.

Hui Chen, https://orcid.org/0000-0001-7020-9668

ACKNOWLEDGEMENT

2022 Hunan Social Science Achievement evaluation committee's topic: "Curriculum carrying ideological and political thinking in the classroom" -- Ideological and political research on College English curriculum based on implicit education theory, Project No.: xsp22ybz096.

REFERENCES

[1] Abdelshaheed, B. S.: Using Flipped Learning Model in Teaching English Language Among Female English Majors in Majmaah University, English Language Teaching, 10(11), 2017, 96-110. https://doi.org/10.5539/elt.v10n11p96

[2] Andrunyk, V.; Shestakevych, T.; Pasichnyk, V.: The Technology of Augmented and Virtual Reality in Teaching Children with ASD, Econtechmod: Scientific Journal, 4 (7), 2018, 7(4), 2018, 59-64.

[3] Ayçiçek, B.; YanparYelken, T.: The Effect of Flipped Classroom Model on Students' Classroom Engagement in Teaching English, International Journal of Instruction, 11(2), 2018, 385-398. https://doi.org/10.12973/iji.2018.11226a

[4] Chang, P. W.; Chen, B. C.; Jones, C. E.; Bunting, K.; Chakraborti, C.; Kahn, M. J.: Virtual Reality Supplemental Teaching at Low-Cost (VRSTL) as a Medical Education Adjunct for Increasing Early Patient Exposure, Medical Science Educator, 28(1), 2018, 3-4. https://doi.org/10.1007/s40670-017-0483-4

[5] Dayarathna, V. L.; Karam, S.; Jaradat, R.; Hamilton, M. A.; Nagahi, M.; Joshi, S.; Driouche, B.: Assessment of the Efficacy and Effectiveness of Virtual Reality Teaching Module: A Gender-Based Comparison, International Journal of Engineering Education, 36(6), 2020, 1938-1955.

[6] Fatimah, A. S.; Santiana, S.; Saputra, Y.: Digital Comic: An Innovation of Using Toondoo as Media Technology For Teaching English Short Story, English Review: Journal of English Education, 7(2), 2019, 101-108. https://doi.org/10.25134/erjee.v7i2.1526

[7] Gupta, A.: Principles and Practices of Teaching English Language Learners, International Education Studies, 12(7), 2019, 49-57. https://doi.org/10.5539/ies.v12n7p49

[8] Guzachchova, N.: Zoom Technology as an Effective Tool for Distance Learning in Teaching English to Medical Students, Bulletin of Science and Practice, 6(5), 2020, 457-460. https://doi.org/10.33619/2414-2948/54/61

[9] Hadi, M. S.: The Use of Song in Teaching English for Junior High School Student, English Language in Focus (ELIF), 1(2), 2019, 107-112. https://doi.org/10.24853/elif.1.2.107-112

[10] Hernandez-Pozas, O.; Carreon-Flores, H.: Teaching International Business Using Virtual Reality, Journal of Teaching in International Business, 30(2), 2019, 196-212. https://doi.org/10.1080/08975930.2019.1663779

[11] Mahboob, A.: 2018, Beyond global Englishes: Teaching English as a dynamic language, RELC journal, 49(1), 36-57. https://doi.org/10.1177/0033688218754944

[12] Mayne, R.; Green, H.: Virtual Reality for Teaching and Learning in Crime Scene Investigation, Science & Justice, 60(5), 2020, 466-472. https://doi.org/10.1016/j.scijus.2020.07.006

[13] McCool, K. E.; Bissett, S. A.; Hill, T. L.; Degernes, L. A.; Hawkins, E. C.: Evaluation of a Human Virtual-Reality Endoscopy Trainer for Teaching Early Endoscopy Skills to Veterinarians, Journal of veterinary medical education, 47(1), 2020, 106-116. https://doi.org/10.3138/jvme.0418-037r

[14] Sundari, H.: Classroom Interaction in Teaching English as Foreign Language at Lower Secondary Schools in Indonesia, Advances in Language and Literary Studies, 8(6), 2017, 147-154. https://doi.org/10.7575/aiac.alls.v.8n.6p.147

[15] Susanty, L.; Hartati, Z.; Sholihin, R.; Syahid, A.; Liriwati, F. Y.: Why English Teaching Truth on Digital Trends as an Effort for Effective Learning and Evaluation: Opportunities and Challenges: Analysis of Teaching English, Linguistics and Culture Review, 5(S1), 2021, 303-316. https://doi.org/10.21744/lingcure.v5nS1.1401

[16] Taubert, M.; Webber, L.; Hamilton, T.; Carr, M.; Harvey, M.: Virtual Reality Videos Used in Undergraduate Palliative and Oncology Medical Teaching: Results of a Pilot Study, BMJ Supportive & Palliative Care, 9(3), 2019, 281-285. https://doi.org/10.1136/bmjspcare-2018-001720

[17] Xu, X.; Guo, P.; Zhai, J.; Zeng, X.: Robotic kinematics Teaching System with Virtual Reality, Remote Control and an On-Site Laboratory, International Journal of Mechanical Engineering Education, 48(3), 2020, 197-220. https://doi.org/10.1177/0306419018807376

[18] Zhang, J.; Zhou, Y.: Study on Interactive Teaching Laboratory Based on Virtual Reality, International Journal of Continuing Engineering Education and Life Long Learning, 30(3), 2020, 313-326. https://doi.org/10.1504/IJCEELL.2020.108543